

*Scientific Paper*Doi: <http://dx.doi.org/10.1590/1809-4430-Eng.Agric.v42n1e20210139/2022>

CORRELATION OF SOIL PHYSICAL ATTRIBUTES WITH FURROWING SHANK STRENGTH AND DEPTH IN A NO-TILL SEEDER

Anderson M. Lenz^{1*}, Marcio F. Maggi¹, Flavio Gurgacz¹,
Douglas Bassegio¹, Marcos V. M. Machado¹

^{1*}Corresponding author. Western Paraná State University - UNIOESTE/ Cascavel - PR, Brasil.
E-mail: andersomm25@gmail.com | ORCID ID: <https://orcid.org/0000-0001-7247-7885>

KEYWORDS

SRP, Farming soil,
soil compaction,
Shank horizontal
strength, Shank
Working depth.

ABSTRACT

Furrowing shank horizontal strength and working depth can be correlated with soil compaction in a no-till sowing. This study aimed to evaluate the correlation of furrowing shank strength and working depth with soil physical properties at two working speeds (1.58 and 1.87 m s⁻¹) and four compaction levels induced by an agricultural tractor (0P, 1P, 3P, and 5P+Ballast), with four repetitions in an RBD. Thereby, we aimed to verify a potential increase in sampling density of soil compaction data. Horizontal strength at 1.58 m s⁻¹ had Pearson correlations ranging from 0.74 to 0.73 with soil penetration resistance (SPR), and from 0.57 to 0.72 with some soil properties collected by volumetric ring. Working depth also correlated with several parameters ranging from 0.49 to 0.81. The highest correlations were verified for the speed of 1.58 m s⁻¹, at which shanks maintained greater depth. This increased soil contact with the shank, hence sensitivity to compaction. Our findings show that furrowing shank horizontal strength and working depth can be used to monitor soil compaction.

INTRODUCTION

In healthy soils, solid particles are arranged to promote satisfactory porosity, which allows water infiltration and storage, as well as to induce plant root development. These soils do not have dense layers, providing good conditions for high crop yields (Barbosa et al., 2020; Melloni et al., 2018; Souza-Lima et al., 2017). Soil physical properties should be evaluated to verify potential needs for mechanical interventions or monitoring cover crop effects (Cho et al., 2015). Physical conditions are commonly evaluated by undeformed samples, in which density, total soil porosity, macroporosity and microporosity are determined (Holthusen et al., 2018).

Another parameter used is Soil Penetration Resistance (SPR), which is measured by a penetrometer and considers soil water content, as it influences soil particle cohesion strength (Ampadu & Fiadjoe, 2015). Stolf et al. (2014) recommended that SPR measurements must be made with soil water content corresponding to or close to field capacity. Moreover, sampling density of SPR and volumetric

ring data collection normally used is one point per hectare (Cherubin et al., 2015). Afterwards, these data are compared with yield maps (Baron et al., 2018), obtained from monitors installed in grain harvesters, which collect a greater amount of data per hectare (Kuiawski et al., 2017). Therefore, methods producing a greater number of soil compaction data can make better comparisons of these parameters.

One parameter affected by changes in soil physical properties is the horizontal strength of furrowing shanks in a no-till system (Conte et al., 2008; Cepik et al., 2010; Troger et al., 2012). Furrowing shanks in fertilizer seeders have the role of opening furrows and depositing fertilizers at a depth of 0.1 to 0.17 m (Nunes et al., 2015). Within this layer, there are the highest soil compaction levels in a no-till system (Silva et al., 2012; Sales et al., 2016). Measurements of furrowing shank horizontal strength must be considered as this parameter is influenced by soil depth, moisture content, and shank-to-soil attack angle (Troger et al., 2012). Horizontal strength of furrowing shanks has been

¹ Universidade Estadual do Oeste do Paraná - UNIOESTE/ Cascavel - PR, Brasil.

Area Editor: Fábio Lúcio Santos

Received in: 8-17-2021

Accepted in: 1-5-2022

commonly measured by installing strain gauges in places where large elastic deformations occur (Conte et al., 2008; Cepik et al., 2010). Up to the proportionality limit of Hooke's law, deformations will be proportional to the applied forces, and strain gauges measure electrical changes proportional to those forces (Rajabi & Hosseini-Hashemi, 2017).

Given the difficulty in collecting SPR data by penetrometers, Cho et al. (2015) and Hemmat et al. (2009) tested a horizontal penetrometer, which consists of a furrowing shank with conical tip or wedge-like tool, whose horizontal force is measured by a load cell while traveling in the soil. Using this force, the horizontal cone index is calculated, measured at one or several depths. This equipment allows collecting more data on soil compaction per unit area. Hemmat et al. (2008) studied the correlation of soil compaction with vertical strength and in-soil depth of cutting discs. They concluded that both parameters are influenced by soil compaction levels.

Our hypothesis was that horizontal strength and working depth of furrowing shanks are correlated with some soil physical properties (apparent density, macro and microporosity, total porosity, and SRP). To this end, we tested two traveling speeds and four soil compaction levels. Our goal was to check whether these two measures could increase the sampling density of soil compaction data in farming areas.

MATERIAL AND METHODS

Equipment instrumentation and assembly

The set-up of collection systems, instrumentation of furrowing shank with the gluing of strain gauges, and calibration were performed at the Laboratory of Agricultural Machinery (LAMA), State University of Western Paraná (UNIOESTE), in Cascavel city, Paraná State (Brazil). The no-till furrowing shank used in the experiment was 0.48 m long and consisted of 2 parts (Figure 1, part 1): a support (C) fixed to the stringer (B) and a movable shank (D) fixed to it by two bolts. These bolts were positioned in such a way that while moving in the soil and

encountering an obstacle such as a stone, for example, the lower bolt, which is designed to serve as a fuse, breaks and causes the furrowing shank (D) to move backwards, preventing damage to other parts. Since there is a moving part, we chose to install strain gauges on the shank support (C) that remains fixed, facilitating the installation of electrical conductors and reducing the need for foldable connections.

The hanging system used to measure the horizontal strength of the furrowing shank was composed of a stringer (Figure 1, part 2) (B) fixed to the structural chassis of the seeder at the coupling point (H). The shank was fixed to the stringer at one end, which is pressed against the soil by the compression force of the spring (I) fixed at the other end, whose depth is restricted by a limiting wheel (E) adjusted to work at 0.15 m depth. When the soil had low compaction, the vertical force of the spring maintained the shank at the depth set by the limiting wheel. The full force of the spring was exerted on the limiting wheel. Thus, changes in shank horizontal strength stemmed from soil compaction or shank working depth variations to which the shank was set. (Conte et al., 2008; Cepik et al., 2010; Sun et al., 2006).

When compaction levels increase, the soil works as a support for the furrowing shank, decreasing the working depth below the 0.15 m adjusted by the limiting wheel. Thus, the spring force (I) is supported on the furrowing shank tip, pressing it against the soil to maintain the intended depth. In seeders, compression springs are used, the more they are compressed, the more force they apply to their ends (Mehendale et. al., 2017).

The force measurement system comprised strain gauges connected to an HX711 load cell amplifier. A potentiometric sensor was used to measure shank depth. Both components were connected to an Arduino Uno board, which records the measurements and saves them in a .csv file on an SD card. For calibration, in both sensors, R^2 was above 0.99. In several weight loading and unloading cycles in the case of the shank, and height lifting and lowering in the case of depth sensor, indicating that there is high quality in the readings.



FIGURE 1. Detailing of the assembly set to measure furrowing shank strength and working depth.

Legend: Cutting disc (A), fixing stringer (B), shank support (C), furrowing shank (D), limiting wheel (E), potentiometric sensor (F), and arm with wheel to contact the soil and measure shank depth (G). Coupling point (H) and compression spring (I).

The shank working depth was measured using a potentiometric sensor (Figure 1) (F) connected to the mobile arm with wheel in contact with the soil (G). This arm (G) was fixed to the stringer (B) where the furrowing shank (C, D) was fixed, which, when entering the working position, limited by the limiting wheel (E) to 0.15 m, moved the arm upwards and rotated the sensor, thus allowing to measure the furrowing shank effective depth. Our depth measurement system was like that of Bölenius et al. (2018).

Design of field collection

The experiment area has been cultivated under no-tillage with rotation of soybeans (*Glycine max*) in spring-summer and corn (*Zea mays*) in summer-autumn for the last 30 years. The area is in the city of Missal, Paraná State (Brazil), with central coordinates of 25° 5' 24.49" S, 54° 13' 51.77" W, and 293-m altitude. The soil is classified as red clayey (Teixeira et al., 2017). Its grain size composition and gravimetric moisture and organic matter contents are shown in Table 1, which were measured by the Solo Análise de Cascavel - PR.

TABLE 1. Grain size composition, gravimetric moisture, and organic matter contents.

Sand (g kg ⁻¹)	Silt (g kg ⁻¹)	Clay (g kg ⁻¹)	Gravimetric moisture (g kg ⁻¹)	Organic matter (g dm ⁻³)
187.5	175	637.5	211.4	39.56

To correlate furrowing shank horizontal strength and working depth with soil physical properties, soil compaction condition was changed by a randomized block experiment in a subplot scheme with four repetitions. The plots consisted of four compaction levels: L1 - with no tractor pass; L2 - one tractor pass weighing 6 Mg (rear wheels 18.4-34 R1 and front wheels 14.9-24 R1, with 3.6 Mg on the rear wheels and 2.4 Mg on the front wheels); L3 - three passes of a 6-Mg tractor; and L4 - five passes of a tractor + ballast (composed of a 500 kg subsoiler) totaling 6.5 Mg with 4.225 Mg on the rear wheels and 2.275 Mg on the front wheels). Initial compaction level in plots was considered to be that of L1. Subplots were constituted by two travel speeds (1.58 and 1.87 m s⁻¹), each subplot had a dimension of 3.8 × 10.5 m.

At each compaction level, two volumetric rings were collected to measure soil bulk density, total porosity,

macroporosity, and microporosity (Gomide et al., 2011) at two depths (0–0.05 and 0.05–0.10 m). These soil layers concentrate the highest soil compaction levels in a no-tillage system (Silva et al., 2012; Sales et al., 2016). Soil resistance to penetration (SRP) was measured at sampling points spaced around 0.50 m from the volumetric ring, using an impact penetrometer to a depth of 0.20 m (Stolf et al., 2014). We made two measurements per point to determine SPR values at every 0.05 m of depth.

Furrowing shank horizontal strength and working depth were measured at two speeds commonly used for seeding (1.58 and 1.87 m s⁻¹), as in figure 2, at a 1 Hz frequency, composing 5 measurements per plot and considering the average for statistics. Induced compaction, collection of undisturbed samples, and sowing took place within a time span of 24 hours.

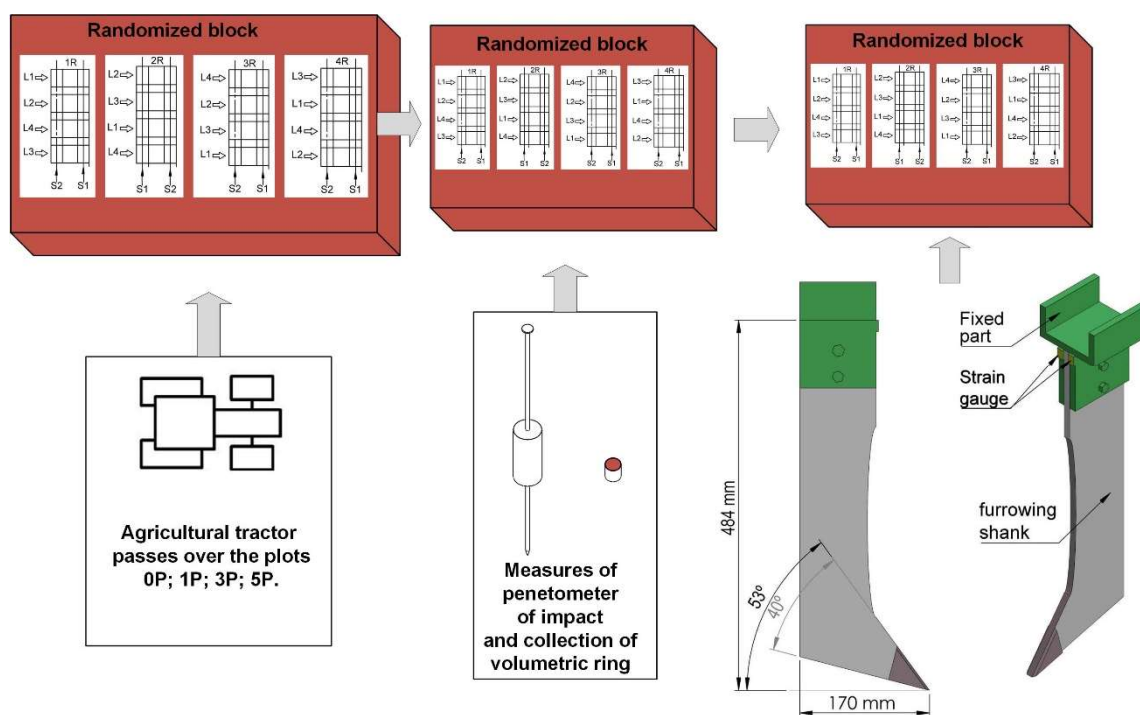


FIGURE 2. Summary of data collection design and analysis.

Horizontal strength and working depth data for two speeds and compaction levels underwent analysis of variance, with means compared by the Tukey's test at 5% error probability. Correlations of working depth and horizontal strength with soil physical properties were analyzed at 5% probability level by the Pearson's correlation test.

RESULTS AND DISCUSSION

Effect of tractor passes

Agricultural tractor passes over the plots significantly affected horizontal strength and working depth of the furrower at both travel speeds (Table 2). The induced compaction caused by the tractor traffic over the plots also affected SRP within the depth ranges of 0–0.05 m and 0.05–0.10 m and macroporosity within the 0–0.05 m range.

TABLE 2. Summary of the analysis of variance for the parameters analyzed as a function of agricultural tractor passes.

Parameter	Average	CV (%)	p Block	p Passes
FSS (N) (1.58 m s ⁻¹)	2620	9.68	0.003**	0.005**
FSS (N) (1.87 m s ⁻¹)	2814	9.04	0.257	0.026*
FSD (m) (1.58 m s ⁻¹)	0.11	6.67	0.406	0.008**
FSD (m) (1.87 m s ⁻¹)	0.10	5.85	0.284	0.001**
SRP MPa (0–0.05 m)	3.64	30.2	0.529	0.001**
SRP MPa (0.05–0.10 m)	4.21	20.6	0.088	0.032*
SRP MPa (0.10–0.15 m)	4.32	25.5	0.318	0.354
SRP MPa (0.15–0.20 m)	4.05	16.6	0.281	0.589
D g / m ⁻³ (0–0.05 m)	1.37	4.73	0.401	0.539
D g / m ⁻³ (0.05–0.10 m)	1.38	2.72	0.887	0.547
Ma% (0–0.05 m)	57	1.17	0.011*	0.023*
Ma% (0.05–0.10 m)	56.6	1.67	0.067	0.443
Mi% (0–0.05 m)	42.8	2.69	0.157	0.099
Mi% (0.05–0.10 m)	43.3	2.18	0.066*	0.443
Pt% (0–0.05 m)	50.9	4.53	0.607	0.913
Pt (0.05–0.10 m)	50.4	3.24	0.190	0.939

Notes: *Significant at 5% probability ($p < 0.05$); **Significant at 1% probability ($p < 0.01$). FSS: Furrowing shank strength; FSD: Furrowing shank depth; SRP: Soil resistance to penetration; D: Soil density; Ma: Macroporosity; Mi: Microporosity; Pt: Total porosity.

Effect of tractor passes on parameters collected by volumetric ring

Macroporosity in the 0–0.05 m depth layer was significantly reduced ($p < 0.05$) as farm tractor passes

increased (Figure 3E). Averages of soil density and microporosity increased (Figure 3A and 3G). As the number of passes increased, macroporosity in the 0.05–0.10 m depth layer also reduced (Figure 3F), while microporosity increased (Figure 3H).

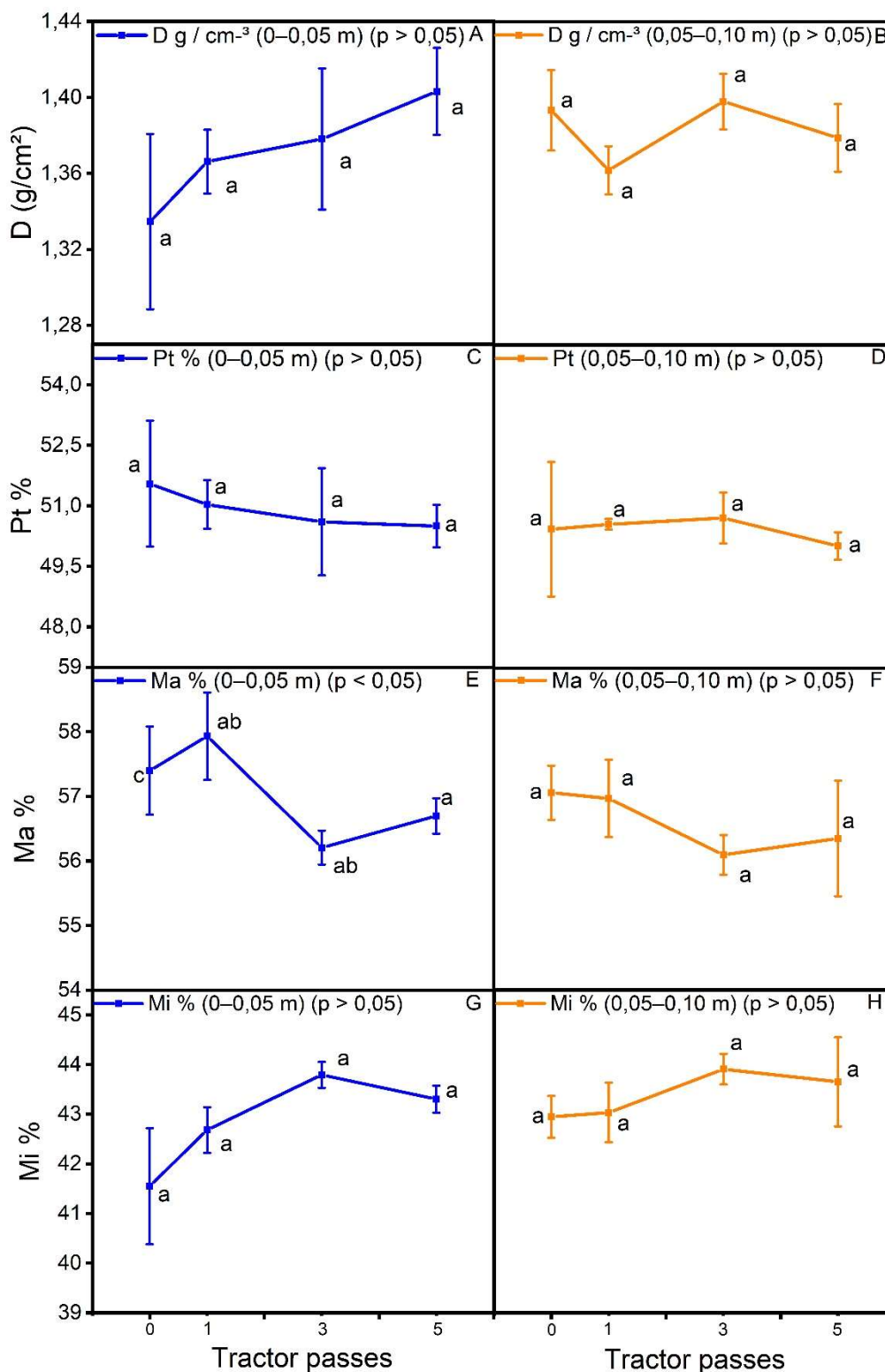


FIGURE 3. Effects of tractor passes on soil physical properties collected by volumetric ring.

Note: Equal letters mean equal averages, at 5% significance by the Tukey's test.

Legend: D: Soil bulk density; Ma: Macroporosity; Mi: Microporosity; Pt: Total porosity.

Effect of tractor passes on SRP

Tractor passes occurred on soil with an average water content of 31% of its total weight. For the clayey soil under study, this is a suitable level for agricultural operations (Molina Junior, 2017). By analyzing the data, we

may see that tractor passes affected SRP levels in the 0–0.05 and 0.05–0.10 m depth layers (Figure 4A and 4B). SRP in the 0–0.05 m layer was most influenced by induced compaction. In the 0.05–0.10 m layer, SRP had similar for 3 and 5 tractor passes (Figure 4).

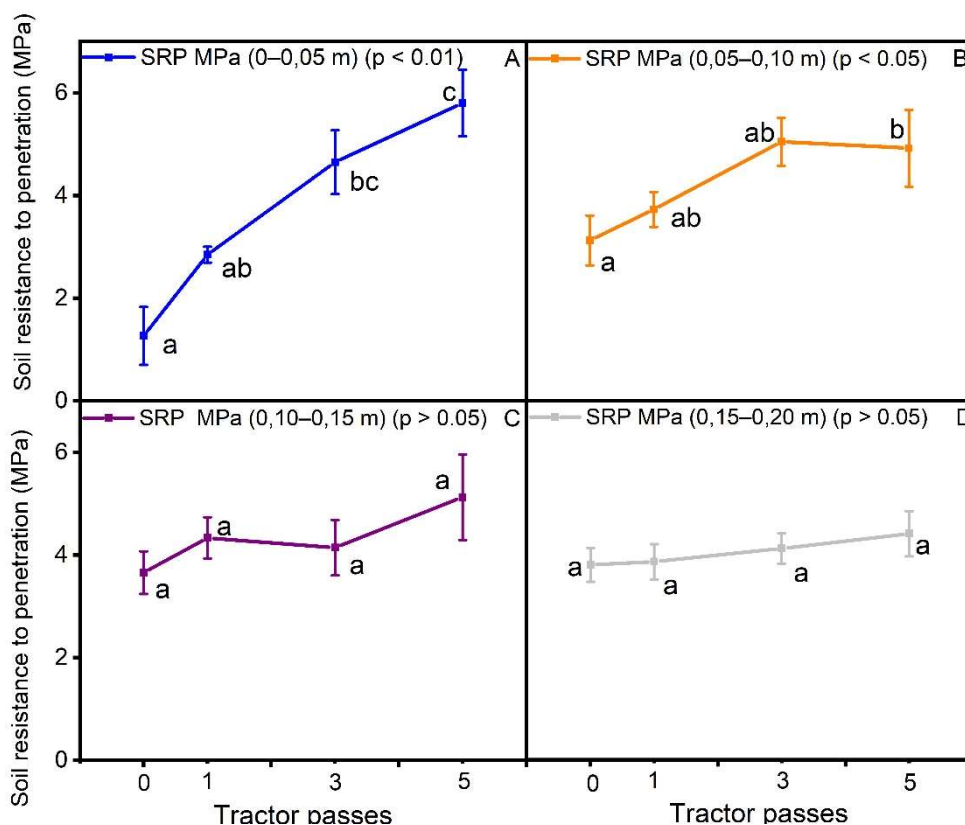


FIGURE 4. Effects of tractor passes on soil resistance to penetration. Notes: Equal letters mean equal averages, at 5% significance by the Tukey's test.

Effect of tractor passes on furrowing shank strength and depth

The *p*-values from analysis of variance and ANOVA construction allowed us to verify that soil compaction by

tractor passes significantly affected (*p*<0.05) the horizontal strength and working depth of furrowing shank. However, travel speed affected significantly (*p*<0.05) only working depth (Table 3).

TABLE 3. *p*-values for furrowing shank horizontal strength and depth.

Source of variation	Horizontal strength	Working depth
Tractor passes	0.0025**	<0.0001**
Travel speed	0.1455	0.0033**
Tractor passes × Travel speed	0.8498	0.366

Notes: *Significant at 5% probability (*p* <0.05); **Significant at 1% probability (*p* <0.01).

The raise in tractor passes from 0 to 5 at 1.58 m s⁻¹ increased shank horizontal strength from 2171 to 3060 N, while at 1.87 m s⁻¹ it was from 2448 to 3068 N (Figure 5A and

5B). Conversely, the raise in tractor passes up to 5 at 1.58 m s⁻¹ decreased shank working depth from 0.12 to 0.10 m, while at 1.87 m s⁻¹ it was from 11.3 to 9.3 m (Figure 5C and 5D).

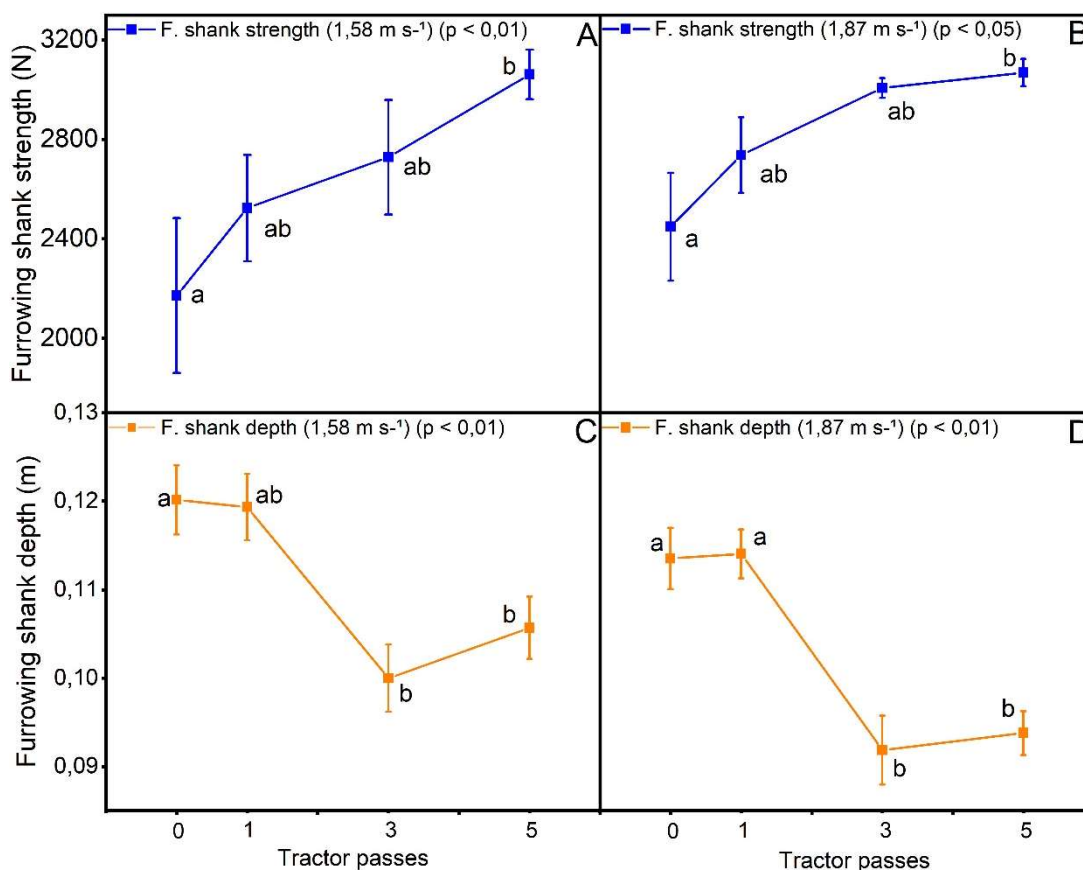


FIGURE 5. Furrowing shank strength and depth after different numbers of tractor passes.

Notes: Equal letters mean equal averages at 5% significance by the Tukey's test.

Silveira et al. (2010) also observed that increasing travel speeds decrease the working depth of furrowing shanks. As speed increased from 1.58 to 1.87 m s⁻¹, working depth averages decreased significantly from 0.11 to 0.10 m (Table 2). Yet the horizontal strength averages were statistically equal at 5% significance at both speeds.

Correlations of soil physical properties with furrowing shank horizontal strength and working depth

In general, horizontal strength at 1.58 m s⁻¹ had more correlations with soil physical properties than at 1.87 m s⁻¹. Working depth showed correlation at both speeds with SRP in the 0–0.05 and 0.05–0.10 m depth layers, and with macroporosity in the 0.05 m depth layer at 1.87 m s⁻¹ (Table 4).

TABLE 4. P – Correlation between strength and depth measurements with soil physical parameters.

Parameter	FSS (N) (1.58 m s ⁻¹)	FSS (N) (1.87 m s ⁻¹)	FSD (m) (1.58 m s ⁻¹)	FSD (m) (1.87 m s ⁻¹)
SRP Mpa (0–0.05 m)	0.001**	0.001**	0.003**	0.003**
SRP Mpa (0.05–0.10 m)	0.128	0.011*	0.038*	0.013*
SRP Mpa (0.10–0.15 m)	0.442	0.161	0.241	0.253
SRP Mpa (0.15–0.20 m)	0.467	0.078	0.246	0.271
Dg m ⁻³ (0–0.05 m)	0.009**	0.054	0.136	0.212
Dg m ⁻³ (0.05–0.10 m)	0.486	0.354	0.069	0.661
Ma% (0–0.05 m)	0.019*	0.769	0.061	0.025*
Ma% (0.05–0.10 m)	0.037*	0.282	0.451	0.117
Mi% (0–0.05 m)	0.001**	0.004**	0.348	0.055
Mi% (0.05–0.10 m)	0.037*	0.282	0.451	0.117
Pt% (0–0.05 m)	0.053	0.383	0.145	0.456
Pt% (0.05–0.10 m)	0.021*	0.103	0.658	0.900

Notes: *Significant at 5% probability (p < 0.05); **Significant at 1% probability (p < 0.01). FSS: Furrowing shank strength; FSD: Furrowing shank depth; SRP: Soil resistance to penetration; D: Soil bulk density; Ma: Macroporosity; Mi: Microporosity; Pt: Total porosity.

At both speeds, in the 0–0.05 and 0.05–0.10 m depth layers, as SRP increased shank horizontal strength increased (Figure 6). The highest correlations were observed in the 0–0.05 m depth layer (Figure 6A). In the 0–0.05 and 0.05–0.10 m depth layers, SRP increases reduced shank working depth,

with higher correlation values ($r = -0.81$) in the 0–0.05 m depth layer. The correlation between SRP and horizontal strength in the 0–0.05 m depth layer was $r = 0.74$ at 1.58 m s^{-1} and $r = 0.73$ at 1.87 m s^{-1} . In the 0.05–0.10 m depth layer, the correlation coefficient was $r = 0.61$ at 1.87 m s^{-1} .

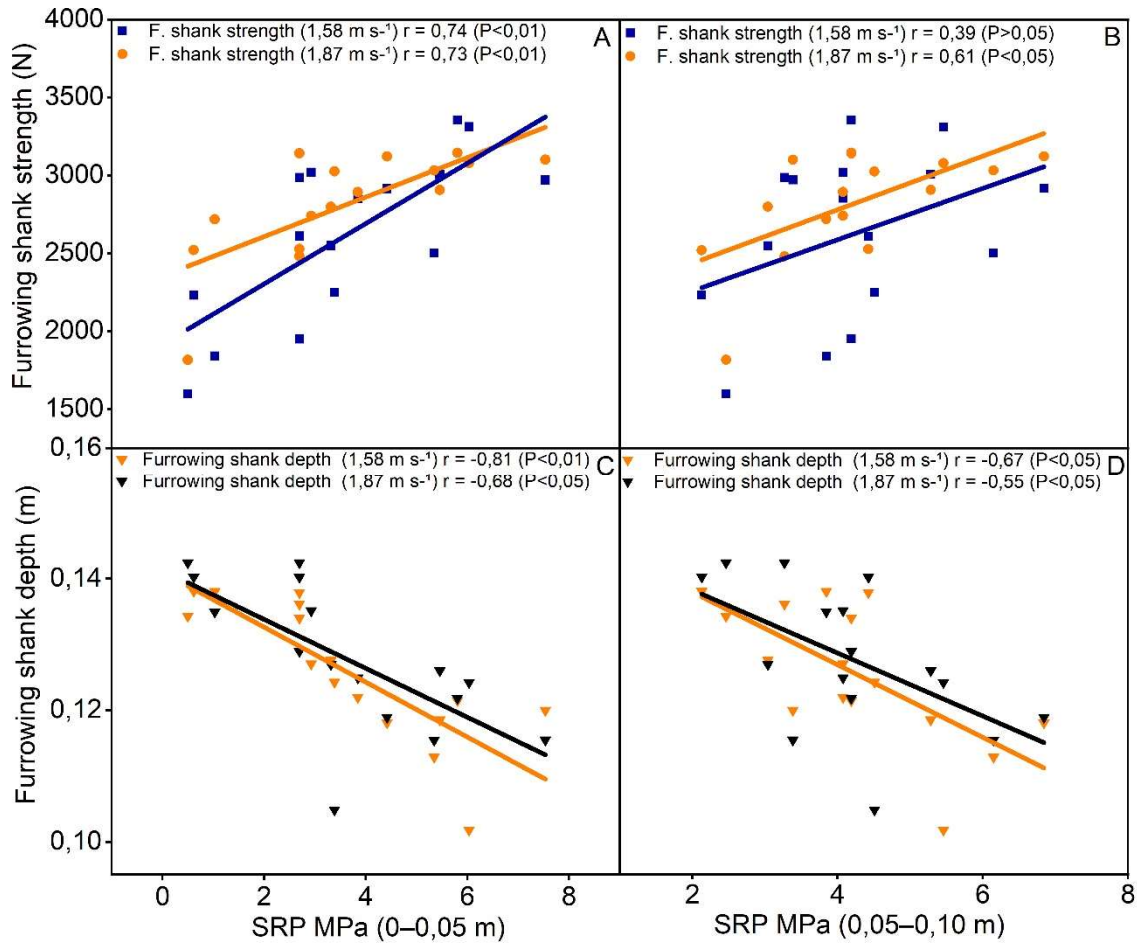


FIGURE 6. Correlation between soil resistance to penetration - SRP (0–0.05 m) and shank horizontal strength (A), SRP (0.05–0.10 m) and shank horizontal strength (B), SRP (0–0.05 m) and shank working depth (C) and SRP (0.05–0.10 m), and shank working depth (D) and shank horizontal strength.

The correlation between horizontal strength and working depth was inverse at both speeds (Figure 7). As working depths increased, shank strength reduced. At 1.58 m s^{-1} , correlation coefficient was $r = -0.62$, while at 1.87

m s^{-1} it was $r = -0.76$. Hemmat et al. (2008) observed a similar effect by analyzing depth and vertical force of cutting discs, in which the deeper the cut, the less vertical force is required.

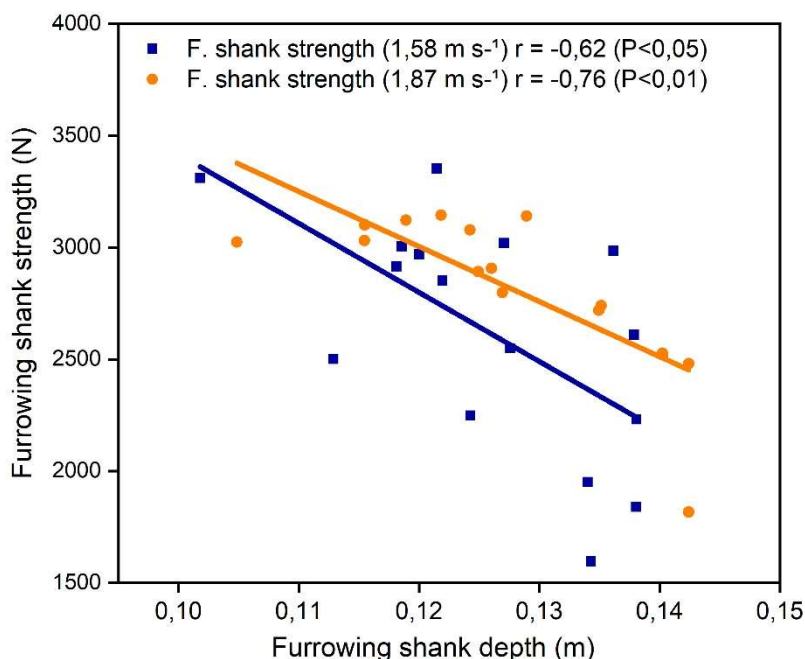


FIGURE 7. Correlation between furrowing shank working depth and horizontal strength at two sowing speeds.

As total porosity in the 0.05–0.10 m soil depth layer increased, shank horizontal strength reduced (Figure 8). Therein, correlation was lower ($r=-0.57$) compared to SRP and in the 0–0.05 m layer ($r=0.74$) (Figure 6). In the 0–

0.05 m depth layer, there was a moderate correlation ($r=-0.64$) between working depth reduction and soil density, and moderate ($r=0.63$) shank strength increase and soil density increase.

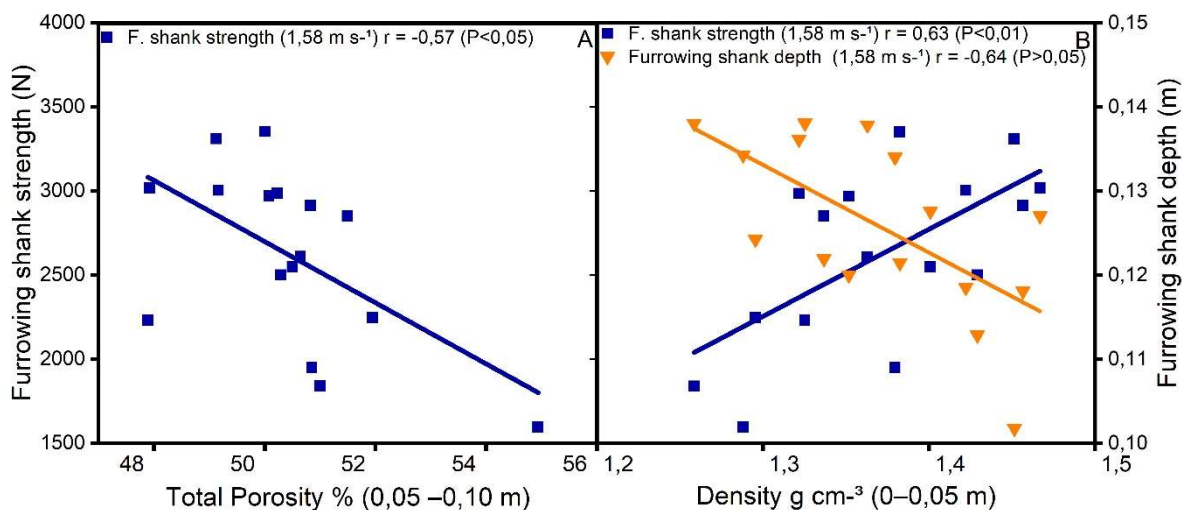


FIGURE 8. Correlation between total porosity and horizontal strength of furrowing shank in the 0.05–0.10 m depth layer (A) and soil density with furrowing shank depth and horizontal strength (B) in the 0–0.05 m depth.

In the 0–0.05 m depth layer, an increase in microporosity raised horizontal strength with a higher correlation ($r=0.72$) at 1.58 m s⁻¹ (Figure 9). Yet macroporosity increase caused a reduction in horizontal strength ($r=-0.57$) and working depth ($r = 0.49$).

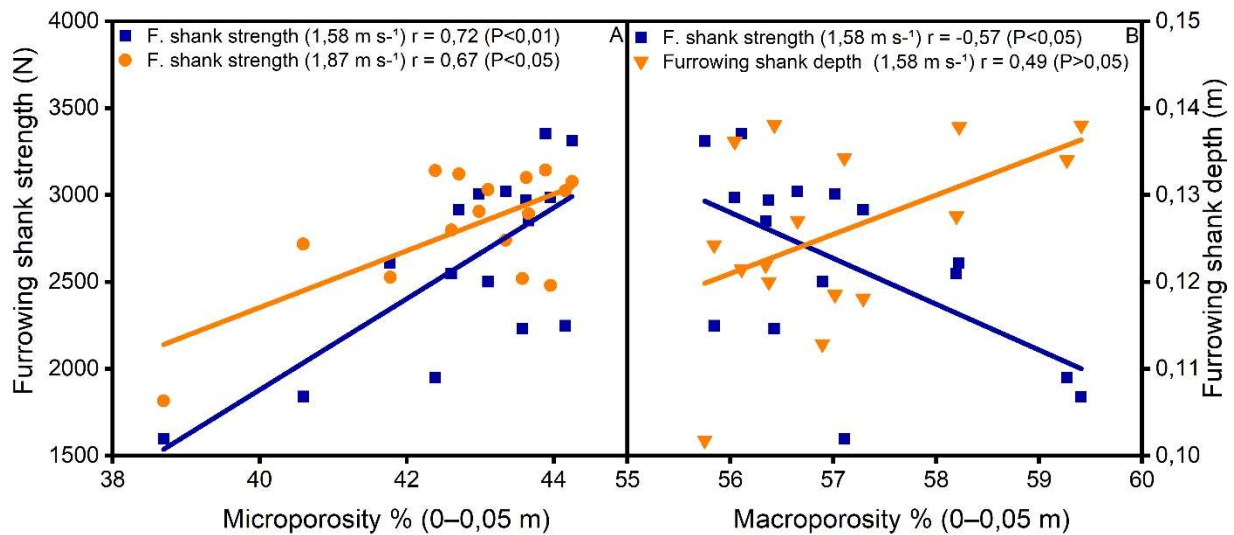


FIGURE 9. (A) Correlation between microporosity (%) in the 0-0.05 m layer with shank horizontal strength. (B) Correlation between macroporosity (%) with shank working depth and horizontal strength in the 0-0.05 m layer.

As tractor passed and hence soil compaction increased, horizontal strength increased and working depth decreased. In other words, the shallower the shank depth, the greater the traction demand, thus showing an inverse correlation (Figures 5, 6, 7). This occurred due to interactions among soil, shank, and spring. During seeder operation, when the shank was pulled over the plots with higher soil bulk density, hardness, and reduced pore space, especially macropores, the furrowing shank had a support that resisted its penetration into the soil. The same occurred with plant roots, mainly during drought or lack of water (Silveira et al., 2011).

The larger furrowing shank support reduced working depth and compressed its suspension spring. Garrido et al. (2011) observed a similar effect as the seeder traveled on more compacted soils, its double seed-metering discs rose to the surface. Hemmat et al. (2008) observed the same behavior for correlation between cutting disc depth and compaction levels, what is characteristic of tilling mechanisms with spring suspension. Spring compression makes the furrowing shank strength against the soil increase, increasing its horizontal force (Mehrabi et al., 2019). Elevation in soil bulk density, which also increases the force applied to the shank, increases tensile demand, which occurs when compaction increases (Conte et al., 2008; Cepik et al., 2010; Sun et al., 2006; Troger et al., 2012).

Soil bulk density averages in the 0–0.05 m depth layer ranged from 1.33 to 1.4 g m⁻³. These values were within the critical density (1.3 to 1.4 g m⁻³) (Reinert et al., 2008; Zhao et al., 2019); therefore, the soil in the plots was compacted. The highest correlations with horizontal strength and with working depth were observed in the 0–0.05 m depth layer. This is because this layer was the most affected by induced compaction thus most influenced traction demand. Valichski et al. (2012) observed that surface layer (0–0.10 m) is the most affected by tractor's induced compaction (5 Mg), and compaction is only up to the fifth pass. Horizontal strength, working depth, and SRP measurements in the 0–0.05 and 0–0.10 m depth layer were more sensitive to the number of tractor passes. agricultural,

with statistical differences for all measures and differences by the Tukey's test.

When the seeder moved at 1.58 m s⁻¹, shank horizontal strength correlated with almost all soil physical properties from volumetric rings. This is the most representative method to determine compaction state with good repeatability of absolute values. Moreover, its measurements are not influenced by soil moisture (Gomide et al., 2011). At 1.58 m s⁻¹, strength correlated with SRP in the 0–0.05 m layer, a method widely used to assess compaction. At 1.87 m s⁻¹, there were lower correlations with parameters measured from volumetric rings.

Despite the small amplitude of parameters collected by volumetric ring (density, total porosity, macro and microporosity) after tractor passes, these indexes correlated with horizontal strength, showing their high sensitivity level. Correlation between horizontal soil resistance by furrowing shank and vertical by SRP is close to the determination coefficients found by Cho et al. (2015) (R²=0.94) and Hemmat et al. (2009) (R²=0.75) and horizontal strength found by Conte et al. (2008) (R²=0.87) and Conte et al. (2008) (R²=0.99). These correlations between the two parameters were expected, as they are similar ways of simulating root effort to penetrate soils and measure its resistance, but one applies the force vertically and the other horizontally.

At 1.58 m s⁻¹, a greater number of correlations were observed since the shank worked deeper. Silveira et al. (2010) and Junior et al. (2000) also observed that, at lower speeds, shank-type furrowers can maintain themselves working at deeper depths. This is because lower speeds make shanks moves within a smaller area per second, providing less support and less resistance to its penetration. Thus, the force that the string exerts on the shank is distributed over a smaller soil volume at a given time interval, and hence manages to keep the shank deeper. As it remains at deeper depths and has a slower displacement, the shank could better sensitize soil compaction changes, increasing the number of correlations.

CONCLUSIONS

Horizontal strength and working depth of furrowing shank correlate with soil physical properties, especially at 1.58 m s⁻¹. Soil compaction increase produced by tractor traffic reduces furrower working depth due to interactions among soil, shank, and spring. Our instrumentation allows collecting shank strength and depth data reliably. The correlations of horizontal strength and depth of furrowing shanks with soil physical properties showed that their monitoring is a feasible alternative to check soil compaction during sowing.

ACKNOWLEDGEMENTS

I thank CAPES for conceiving a doctoral scholarship, which made it possible to carry out this study.

REFERENCES

- Ampadu SIK, Fiadjoe GJY (2015) The influence of water content on the Dynamic Cone Penetration Index of a lateritic soil stabilized with various percentages of a quarry by-product. *Transportation Geotechnics* 5: 68-85. DOI: <https://doi.org/10.1016/j.trgeo.2015.09.007>.
- Barbosa TDCS, Costa NMGB da, Santos DB dos, Machado MS, Marques Filho F (2020) Qualidade física do solo em áreas sob manejo agroecológico e convencional. *Brazilian Journal of Development* 6(7): 48899-48909. DOI: <https://doi.org/10.34117/bjdv6n7-511>
- Baron FA, Corassa Junior GM, Fioresi D, Santi AL, Martini RT, Kulczynski SM (2018) Qualidade fisiológica de sementes de soja em diferentes ambientes de produtividade e densidade de plantas. *Revista Brasileira de Engenharia Agrícola e Ambiental* 22(4):237-242. DOI: <https://doi.org/10.1590/1807-1929/agriambi.v22n4p237-242>
- Bölenius E, Wetterlind J, Keller T (2018) Can within field yield variation be explained using horizontal penetrometer resistance and electrical conductivity measurements? Results from three Swedish fields. *Acta Agriculturae Scandinavica, Section B—Soil & Plant Science* 68:(8)690-700. DOI: <https://doi.org/10.1080/09064710.2018.1464201>.
- Cepik CT, Trein CR, Levien R, Conte O (2010) Força de tração e mobilização do solo por hastes sulcadoras de semadoras-adubadoras. *Revista Brasileira de Engenharia Agrícola e Ambiental* 14: 561-566. DOI: <https://dx.doi.org/10.1590/S1415-43662010000500015>
- Cherubin MR, Santi AL, Eitelwein MT, Amado TJC, Simon DH, Damian JM (2015) Dimensão da malha amostral para caracterização da variabilidade espacial de fósforo e potássio em Latossolo Vermelho. *Pesquisa Agropecuária Brasileira* 50:168-177. DOI: <https://dx.doi.org/10.1590/S0100-204X2015000200009>
- Cho Y, Lee DH, Park W, Lee KS (2015) Development of a Real-Time Measurement System for Horizontal Soil Strength. *Journal of Biosystems Engineering* 40(3):165-177. DOI: <http://dx.doi.org/10.5307/jbe.2015.40.3.165>
- Conte O, Levien R, Trein CR, Mazurana M, Debiasi H (2008) Resistência mecânica do solo e força de tração em hastes sulcadoras de semadoras-adubadoras em sistema de integração lavoura-pecuária. *Engenharia Agrícola* 28(3):730-739. DOI: <http://dx.doi.org/10.1590/s0100-69162008000400013>
- Garrido M, Conceição LA, Baguena EM, Valero C, Barreiro P (2011) Evaluating the need for an active depth-control system for direct seeding in Portugal. In *Proceedings of the 8th European Conference on Precision Agriculture*. Wageningen, Academic Publishers, Proceedings...
- Gomide PHO, Silva MLN, Soares CRFS (2011) Atributos físicos, químicos e biológicos do solo em ambientes de voçorocas no município de Lavras-MG. *Revista Brasileira de Ciência do Solo* 35: 567-577. DOI: <https://dx.doi.org/10.1590/S0100-06832011000200026>
- Hemmat A, Adamchuk VI, Jasa P (2008) Use of an instrumented disc coulter for mapping soil mechanical resistance. *Soil and Tillage Research* 98(2): 150-163. DOI: <https://doi.org/10.1016/j.still.2007.11.003>
- Hemmat A, Khorsandy A, Masoumi AA, Adamchuk VI (2009) Influence of failure mode induced by a horizontally operated single-tip penetrometer on measured soil resistance. *Soil and Tillage Research* 105(1): 49-54. DOI: <http://dx.doi.org/10.1016/j.still.2009.05.003>
- Holthusen D, Brandt AA, Reichert JM, Horn R (2018) Soil porosity, permeability and static and dynamic strength parameters under native forest/grassland compared to no-tillage cropping. *Soil and Tillage Research* 177: 113-124. DOI: <https://doi.org/10.1016/j.still.2017.12.003>
- Junior RC, Araújo AGD, Ralisch R (2000) Desempenho da semeadora-adubadora MAGNUM 2850 em plantio direto no basalto paranaense. *Pesquisa Agropecuária Brasileira* 35: 523-532. DOI: <http://dx.doi.org/10.1590/s0100-204x2000000300007>.
- Kuiawski ACMB, Safanelli JL, Bottega EL, Oliveira AMD, Guerra N (2017) Vegetation indexes and delineation of management zones for soybean I. *Pesquisa Agropecuária Tropical* 47: 168-177. DOI: <https://doi.org/10.1590/1983-40632016v4743904>
- Mehendale S, Bambole A, Raghunath S (2017). Desenvolvimento de elemento de interface para modelagem de alvenaria estrutural. *Revista ALCONPAT* 7(1):00007. DOI: <https://doi.org/10.21041/ra.v7i1.147>
- Mehrabani MH, Ibrahim Z, Ghodsi SS, Suhatri M (2019) Seismic characteristics of X-cable braced frames bundled with a pre-compressed spring. *Soil Dynamics and Earthquake Engineering* 116: 732-746. DOI: <https://doi.org/10.1016/j.soildyn.2018.10.014>

Melloni R, Costa NR, Melloni EGP, Lemes MCS, Alvarenga MIN, Nunes J (2018) Sistemas agroflorestais cafeeiro-arauária e seu efeito na microbiota do solo e seus processos. *Ciência Florestal* 28: 784-795. DOI: <https://doi.org/10.5902/1980509832392>

Molina Junior, WF (2017) Comportamento mecânico do solo em operações agrícolas. Piracicaba, ESALQ/USP. DOI: <https://doi.org/10.11606/9788592238407>

Nunes MR, Denardin JE, Pauletto EA, Faganello A, Pinto LFS (2015) Mitigation of clayey soil compaction managed under no-tillage. *Soil and Tillage Research* 148:119-126. DOI: <https://doi.org/10.1016/j.still.2014.12.007>

Rajabi K, Hosseini-Hashemi S (2017) Application of the generalized Hooke's law for viscoelastic materials (ghvms) in nonlocal free damped vibration analysis of viscoelastic orthotropic nanoplates. *International Journal of Mechanical Sciences* 124:158-165. DOI: <https://doi.org/10.1016/j.ijmecsci.2017.02.025>

Reinert DJ, Albuquerque JA, Reichert JM, Aita C, Andrada MMC (2008) Limites críticos de Soil bulk density para o crescimento de raízes de plantas de cobertura em Argissolo Vermelho. *Revista Brasileira de Ciência do Solo* 32: 1805-1816. DOI: <http://dx.doi.org/10.1590/s0100-06832008000500002>

Sales RP, Portugal AF, Moreira JAA, Kondo MK, Pegoraro RF (2016) Qualidade física de um Latossolo sob plantio direto e preparo convencional no semiárido. *Revista Ciência Agronômica* 47: 429-438. DOI: <https://dx.doi.org/10.5935/1806-6690.20160052>

Silva SGC, Silva ÁPD, Giarola NFB, Tormena CA, Sá JCDM (2012) Temporary effect of chiseling on the compaction of a Rhodic Hapludox under no-tillage. *Revista Brasileira de Ciência do Solo* 36: 547-555. DOI: <https://dx.doi.org/10.1590/S0100-06832012000200024>

Silveira DDC, Melo Filho JFD, Sacramento JAASD, Silveira ECP (2010) Relação umidade versus resistência à penetração para um Argissolo Amarelo distrocioso no recôncavo da Bahia. *Revista Brasileira de Ciência do Solo* 34:659-667. DOI: <http://dx.doi.org/10.1590/s0100-06832010000300007>

Silveira JCM da, Fernandes HC, Modolo AJ, Lima Silva S de, Trogello E (2011) Furrow depth, soil disturbance area and draft force of a seeder-fertilizer at different seeding speeds. *Revista Ceres* 58(3): 293-298. DOI: <https://doi.org/10.1590/S0034-737X2011000300008>

Souza-Lima ED, Henrique-Lovera L, Montanari R, Panosso AR, Aguilera-Esteban DA (2017) Relações entre componentes morfológicos do palmito e atributos físicos de um inceptisolo: uma abordagem multivariada. *Agricultural Science and Technology* 18(3): 543-554. DOI: https://doi.org/10.21930/rcta.vol18_num3_art:743

Stolf R, Murakami JH, Brugnaro C, Silva LG, Silva LCFD, Margarido LAC (2014) Penetrômetro de impacto stolf-programa computacional de dados em EXCEL-VBA. *Revista Brasileira de Ciência do Solo* 38:774-782. DOI: <https://dx.doi.org/10.1590/S0100-06832014000300009>

Sun Y, Ma D, Lammers PS, Schmittmann O, Rose M (2006) On-the-go measurement of soil water content and mechanical resistance by a combined horizontal penetrometer. *Soil and tillage Research* 86(2):209-217. DOI: <https://doi.org/10.1016/j.still.2005.02.022>

Teixeira PC, Donagemma GK, Fontana A, Teixeira WG (2017) Manual de métodos de análise de solo. Brasília, Embrapa, 573p.

Troger HC, Reis ÂVD, Machado AL, Machado RL (2012) Analyzing the efforts in furrow openers used in low power planters. *Engenharia Agrícola* 32(6):1133-1143. DOI: <https://dx.doi.org/10.1590/S0100-69162012000600015>

Valicheski RR, Grossklaus F, Stürmer SL, Tramontin AL, Baade ES (2012) Desenvolvimento de plantas de cobertura e produtividade da soja conforme atributos físicos em solo compactado. *Revista Brasileira de Engenharia Agrícola e Ambiental* 16: 969-977. DOI: <https://dx.doi.org/10.1590/S1415-43662012000900007>

Zhao C, Chai Q, Cao W, Whalen JK, Zhao L, Cai L (2019) No-tillage reduces competition and enhances compensatory growth of maize (*Zea mays* L.) Intercropped with pea (*Pisum sativum* L.). *Field Crops Research* 243: 107611. DOI: <https://doi.org/10.1016/j.fcr.2019.107611>